

Identification of Key Genes and FUNCTIONAL Pathway in Radioresistance of Non-Small Cell Lung Cancer

Shouying Li^{1,*}, Jiaxin Feng^{2,*}, Haiyan Weng¹, Feng Zhao³, Guohui Cui¹, Wenkui Fu¹, Xiaorong Lin⁴, Hai Hu^{1,5}

¹Department of Oncology, Sun Yat-sen Memorial Hospital, Sun Yat-sen University, Guangzhou, People's Republic of China; ²The First Affiliated Hospital of Guangzhou Medical University, Guangzhou, People's Republic of China; ³Research and Development Department, Guangzhou BioBlue Technology Co. Ltd, Guangzhou, People's Republic of China; ⁴Diagnosis and Treatment Center of Breast Diseases, Shantou Central Hospital, Shantou, People's Republic of China; ⁵Guangdong Provincial Key Laboratory of Malignant Tumor Epigenetics and Gene Regulation, Guangdong-Hong Kong Joint Laboratory for RNA Medicine, Medical Research Center, Sun Yat-Sen Memorial Hospital, Sun Yat-Sen University, Guangzhou, People's Republic of China

*These authors contributed equally to this work

Correspondence: Xiaorong Lin; Hai Hu, Email clarelynn_lin@163.com; huhai@mail.sysu.edu.cn

Purpose: For better understanding of radiotherapy resistance and its potential mechanism.

Methods: We established radioresistance cell lines of non-small cell lung cancer (NSCLC) followed by microarray analysis. 529 differentially expressed genes (DEGs) were then screened between radiation resistant cell lines compared with the sensitive cell lines. The biological functions and enrichment pathways of the above DEGs were identified using Kyoto Encyclopedia of Genes and Genomes (KEGG) and gene ontology (GO) enrichment analyses. Gene Set Enrichment Analysis (GSEA) revealed that the radiation resistance group had the most gene sets enriched in altered immune response, such as TNF signaling pathway, when compared to the radiation sensitive group. Protein-protein interaction (PPI) network was carried out through the STRING database, and then five hub genes (CXCL10, IFIH1, DDX58, CXCL11, RSAD2) were screened by Cytoscape software. RT-PCR confirmed the expression of the above hub genes. ChIP-X Enrichment Analysis showed that STAT1 might be the transcription factor of the above hub genes. Considering that PD-L1 could be activated by STAT1 in a variety of tumors and ultimately lead to immune exhaustion, RT-PCR and Western blot verified the expression level of PD-L1.

Results: Five hub genes (CXCL10, IFIH1, DDX58, CXCL11, RSAD2) were screened and verified to be highly expressed in radioresistance group, STAT1 might be the transcription factor of the above hub genes. Our study found that the expression level of PD-L1 was increased after radiotherapy resistance.

Conclusion: Although immune system activation occurs followed by radiation resistance, we hypothesized that the upregulation of PD-L1 expression caused by STAT1 activation might be one of the mechanisms of radiotherapy resistance.

Keywords: NSCLC, radioresistance, DEGs, hub gene, STAT1

Introduction

Lung cancer is one of the most common and lethal cancers worldwide. Compared with small cell lung cancer (SCLC), the proportion of NSCLC is even higher. Therefore, improving the existing treatment regimen as well as improving survival rate of patients with NSCLC has become the focus of tumor prevention and treatment. Radiotherapy is still one of the preferred treatment options for advanced NSCLC. However, as NSCLC patients are usually accompanied by varying degrees of radiotherapy resistance, which limits the efficacy of tumor radiotherapy, and thus radioresistance has become one of the primary causes for the treatment failure of NSCLC patients. Hence, it is critical to propose the meaningful mechanism of radiotherapy resistance in NSCLC in order to develop new treatment strategies.

At present, the research focus of radiotherapy resistance of NSCLC at home and abroad mainly focuses on PI3K/AKT/mTOR signaling pathway,¹ tumor stem cells (CSCs),² microRNA (miRNA)³ and hepatocyte growth factor receptor (HGF/c-MET).⁴ Despite the above studies, there is still no unified solution. A recent study reported that tumor microenvironment (TME) factors are major barriers to effective radiotherapy.⁵ In addition, activation of inflammatory pathways has been reported to take part in tumor radiation resistance,⁶ especially the IFN/STAT1 pathway.⁷ Previous studies have found that abnormal activation of STAT1 leads to radiation resistance in a variety of cancers, including breast cancer,⁸ human head and neck squamous cell carcinoma,⁹ myeloma,¹⁰ and renal cell carcinoma.¹¹ Besides, PD-L1 expression was reported to be increased in mice following ionizing irradiation,¹² and acquired radiation resistance can be overcome by concurrent PD-L1 blockade in mice.¹³ These studies indicated that the interaction between tumor and immune microenvironment was important in radiation resistance.

In order to better understand the mechanism of radiotherapy resistance and explore new treatment options, we carried out a targeted RNA microarray to screen DEGs. The potential mechanisms of radiotherapy resistance such as cytokine-cytokine receptor interaction was explored with the performance of GO and KEGG pathway analysis as well as PPI network. Five hub genes were screened by Cytoscape. Most of these genes could be activated by IFN- γ and involved in the response of innate immune. Further analysis revealed that STAT1 may be the transcription factor responsible for the upregulation of the hub genes. In addition, we also found that the expression of PD-L1 was significantly increased after the occurrence of radiotherapy resistance. Immune checkpoint inhibitors targeting PD-L1 have shown potent clinical efficacy and have revolutionized the treatment protocols of a broad spectrum of tumor types, especially NSCLC. Preclinical and clinical trials have demonstrated that radiotherapy could induce a systemic antitumor immune response and have a great potential to sensitize refractory “cold” tumors to immunotherapy.¹⁴ Thus, PD-L1 mAb combined with SBRT instead of conventional radiotherapy might be more promising to fight against NSCLC. Our findings indicated that aberrant activation of STAT1 signaling as well as upregulation of PD-L1 may play a role in radioresistance, which revealed the exhaustion of anti-tumor immunity may be one of the mechanisms of radiotherapy resistance in NSCLC.

Materials and Methods

Microarray Data

In this study, lung cancer radiotherapy resistant cells were established by continuous induction of clinical dose gradient increase, lung adenocarcinoma cell line A549 was purchased from the ATCC, and the specific steps were as follows: The lung cancer cell line A549 in logarithmic growth phase was irradiated with 4 Gy for the first time and cultured for subculture. After cell adherence growth, the cells were irradiated again with 4 Gy, with a total dose of 60Gy. The radiotherapy resistance cell line A549-RR was obtained by further culture. Irradiation of 0, 2, 4, 6 and 8Gy (corresponding to inoculated cell numbers are 500, 1000, 2000, 4000 and 8000, respectively). After 2 weeks of cultivation, the clone formation experiment was fixed with 4% paraformaldehyde and then stained with crystal violet. Manual colony count (> 50). Each experiment was repeated at least three times.

Total RNA of cultured cells was isolated using TRIzol reagent (Invitrogen), and the samples were sent to Shanghai Kangcheng Biological Co LTD for RNA microarray analysis.

DEG Screening

The expression levels of case and control samples were normalized by DESeq2 (version 1.22.2). The “limma” package were then used to screen DEGs. Criteria for screening DEGs between different groups: $|\log_{2}FC| > 1$, $p < 0.05$.

GO and Pathway Enrichment Analyses Analysis

KEGG pathway and GO enrichment analysis were conducted by Shanghai Kangcheng Biological Co LTD. Pathway analysis of mRNA expression profiling was carried out by GSEA software. GSEA results are shown as enrichment scores (ES), which reflect the extent to which a set of genes is over-represented at the top or bottom of the sequencing list.

PPI Network and Hub Gene Identification

The building of PPI network was performed using the Search Tool for the Retrieval of Interacting Genes (STRING database; <https://string-db.org/>). The screening criteria are as follows: gene count > 2, adjusted p value < 0.01 and a cut-off point above 0.4 as the interaction score. The first 100 genes were selected for PPI network. To explore hub genes in our study, Cytoscape 3.8.2 was used to enter Cytohubba module with top nodes ranked by MCC to calculate hub genes in the whole PPI network, as reported, MCC performed better than other calculate methods.¹⁵ According to the precise calculation formula reported in the literature, it is more accurate when the number of key genes is small, so we selected top 5 nodes ranked by MCC to calculate hub genes.

Validation of Hub Genes

To further confirm the expression differences of the five hub genes between two samples compared with the results of the microarray analysis, we isolated total RNA from two cell lines. PrimeScript RT reagent kit was applied for reverse transcription of total RNA (Takara, Dalian). SYBR Green Premix Ex Taq (Takara, Japan) was used for cDNA amplification for qRT-PCR. Each experiment was repeated at least three times. The 2DDCt method was used to analyze the data, with ACTB serving as the internal control. Table 1 lists the primers used in qRT-PCR.

The supernatant of cell culture medium was taken and centrifuged at 1000RPM for 5 min. ELISA kit was used to detect the concentrations of cytokines (CXCL10, Absin, abs510027; CXCL11, Elabscience, E-EL-H0051c) using double antibody sandwich method. The supernatant containing cytokines was added to a microtiter plate containing captured antibodies for incubation. The cytokines in the supernatant were captured by solid phase antibody labeled with horseradish peroxidase (HRP) to form an antigen-enzyme-labeled antibody complex, TMB (3,3', 5,5'-tetramylbenzidine) substrate was added for staining. Finally, a stop solution was appended to stop the reaction. The OD value was quantified at 450 nm by Thermo MK3 and then we calculated the concentration according to the absorbance and standard curve.

Analysis of Immune Infiltration Validation of Hub Genes

The “Immune-Gene” module of TIMER2 web server was used to analyze the correlation between hub gene expression and immune infiltrates in all TCGA samples. CD8+ T-cell immune cells were chosen. TIMER, MCPOUNTER, CIBERSORT-ABS, QUANTISEQ, and XCELL algorithms was used to estimate immune infiltration. The p values and partial correlation (cor) values were tested by Spearman rank correlation test with purity adjustment. The data was represented graphically by a heatmap followed by scatter plot.

To verify the above results, we extracted human peripheral blood mononuclear cells for further exploration. Mononuclear cells were isolated with human mononuclear cell separation solution (Haoyang biological, Tianjin, LST1077) following the instructions of manufacturer. Mononuclear cells were cultivated in the upper chamber of transwell in a 24-well plate, and the lower layer was inoculated with tumor cells. The supernatant of tumor cells was collected after 24 hours, followed by centrifugation at 1000g for 5 min. Then cells were re-suspended with PBS, and

Table 1 Primers for Validation

Genes	Forward Primer	Reverse Primer
<i>β-actin</i>	CTACCTCATGAAGATCCTCACCGA	TTCTCCTTAATGTCACGCACGATT
<i>CXCL10</i>	GTGGCATTCAAGGAGTACCTC	TGATGGCCTTCGATTCTGGATT
<i>CXCL11</i>	GACGCTGTCTTTGCATAGGC	GGATTTAGGCATCGTTGTCTTTT
<i>IFIH1</i>	TCGAATGGGTATTCCACAGACG	GTGGCGACTGTCCTCTGAA
<i>DDX58</i>	CTGGACCCTACCTACATCCTG	GGCATCCAAAAGCCACGG
<i>RSAD2</i>	TTGGACATTCTCGCTATCTCCT	AGTGCTTTGATCTGTTCCGTC
<i>PD-L1</i>	GCTGCACTAATTGTCTATTGGGA	AATTCGCTTGATGTCGGCACC

corresponding antibodies (CD3, 560835; CD8, 555367; CD45, 555482, BD Bioscience, 1:100) were added for incubation. Cells were subsequently analyzed with multicolor flow cytometry (BD, FACS Verse). CD3 was primarily used to label T lymphocytes, CD45 was used to label regulatory T cells, CD3, CD8 and CD45 co-staining used for flow cytometry were in order to more accurately label CD8+ T cells. Both CD3 and CD8 positive and CD45 negative cells were selected as experimental subjects. Each experiment was carried out at least three times. All blood samples were obtained with the informed consent of the study participants.

ChIP-X Enrichment Analysis

Input the five hub genes into <https://maayanlab.cloud/chea3/>¹⁶ choose transcription factors that cover all hub genes and reorder transcription factors according to the mean rank.

Immunoblotting

RIPA buffer was used to extract protein and then separated by SDS-polyacrylamide gel, after that protein were transferred to PVDF membrane. Antibodies were as following: anti-STAT1 (9172, 1:1000, Cell Signaling Technology, USA), anti-phospho-STAT1 (9167, 1:1000, Cell Signaling Technology, USA), anti-PD-L1 (A18103, 1:1000, ABclonal, USA) and anti- β -actin (66009, 1:2000, Proteintech, USA). Peroxidase-conjugated secondary antibody (ab6721, 1:1000, Abcam, UK) was used and enhanced chemiluminescence assays (ECL, Thermo) were used to detect the antigen-antibody reactions.

Statistical Analysis

All statistical analyses were performed with GraphPad Prism 9.0. Relative results were displayed as mean \pm mean standard error. To compare the two groups of data, a student's *t*-test was carried out. Statistical significance criteria: $p < 0.05$. * $p < 0.05$, ** $p < 0.01$, and *** $p < 0.001$.

Results

Establishment of Radiotherapy Resistant Cell Lines

Figure 1A shows the diagram of the establishment of radiation resistant cells. Our results showed that the clone formation ability of A549-RR was significantly stronger than that of A549 under the same dose irradiation (Figure 1B and C), and the cell dose survival curve suggested that the survival fraction of A549-RR was obviously higher than that of A549 ($p = 0.0371$, Figure 1D). To identify DEGs between case and control subjects, we constructed A549 radiotherapy resistant cell line followed by microarray analysis. After integration and standardization of the microarray data, 529 DEGs were screened (adjusted $p < 0.05$, $|\logFC| > 1$) as shown in the heatmap (Figure 1E). Among them, 390 upregulated genes and 139 downregulated genes are illustrated in Figure 1F as volcano plots.

Functional Analysis of DEGs

For upregulated genes, GO analysis suggested the most enriched biological process term was related to cytokine activity (GO:0005125), and the receptor regulator activity (GO: 0030545) were secondly enriched in those profile. Extracellular space (GO:0005615) was identified as the most enriched cellular component term. The enriched molecular function term was significantly related to immune response (GO:0006955) and immune effector process (GO:0002252) (Figure 2A). KEGG analysis indicated that the 390 upregulated genes were mainly enriched in cytokine-cytokine receptor interaction (Figure 2B). For downregulated genes, GO analysis showed that the 139 downregulated genes were mainly enriched in tubulin binding, chromosome segregation, and cell division (Figure 2C), KEGG analysis showed that the DEGs were mainly enriched in TGF- β signaling pathway (Figure 2D). The upregulated genes were more enriched in NOD-like receptor signaling pathway, TNF signaling pathway and necroptosis, which were established by gene set enrichment analysis (Figure 2E-G).

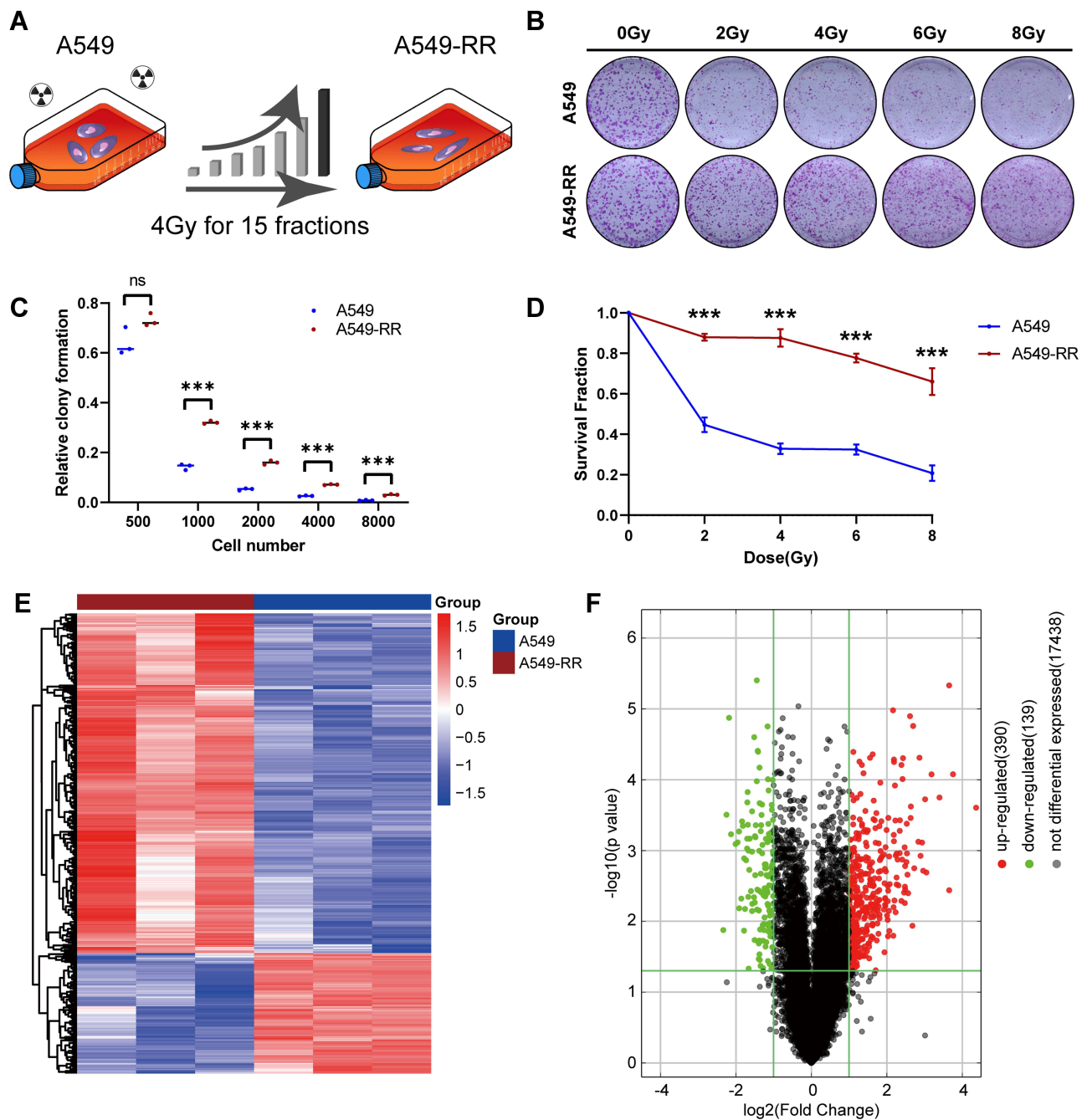


Figure 1 Establishment of radiotherapy resistant cell line. **(A)** The diagram of establishment of radiotherapy resistant cells. **(B)** X ray irradiation of 0, 2, 4, 6 and 8Gy. After 2 weeks of cultivation, then fixed with 4% paraformaldehyde and stained with crystal violet in the colony formation experiment. **(C)** Clone formation rate according to B, the results were calculated according to the ratio of clone number to inoculated cell number. **(D)** Survival fraction according to B. **(E)** Heatmap of DEGs screened by microarray analysis, red areas represent highly expressed genes and blue areas represent lowly expressed genes in A549-RR subjects compared with A549 subjects. **(F)** Differential gene volcano map between the case and control group. The dotted line indicates $p = 0.05$. $***p < 0.001$.
Abbreviations: DEG, differentially expressed gene; ns, no significance.

PPI Network and Hub Gene Screening

Due to the higher proportion of upregulated DEGs and more beneficial to the application of future targets. We mainly analyzed the upregulated genes in this part. PPI network was carried out by STRING database (Figure 3A). Among the 390 genes included, five hub genes (CXCL10, IFIH1, DDX58, CXCL11, RSAD2) were discovered using CytoHubba based on node score ranking using topological analysis of the maximal clique centrality algorithm and the maximum correlation criterion via the CytoHubba plugin of Cytoscape (Figure 3B).

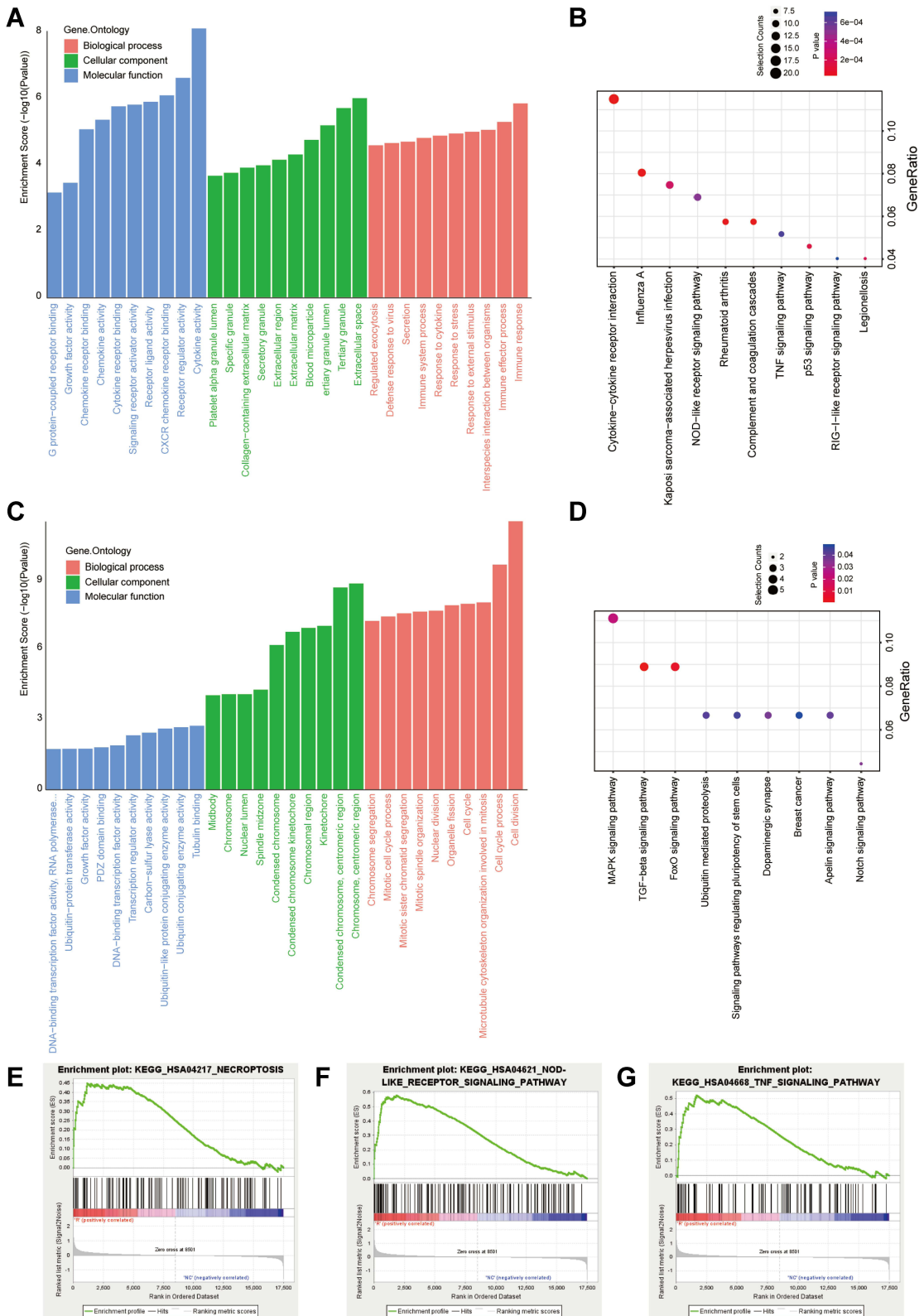


Figure 2 Function and mechanism analysis of altered expression of DEGs. **(A)** GO analysis of the up regulated DEGs. **(B)** KEGG pathway analysis of the up regulated DEGs. **(C)** GO analysis of the down regulated DEGs. **(D)** KEGG pathway analysis of the down regulated DEGs. The top-three most significant up-regulated enriched gene sets in the resistance subjects: NOD-like receptor signaling pathway **(E)**, TNF signaling pathway **(F)**, Necroptosis **(G)**. **Abbreviations:** DEG, differentially expressed gene. BP, Biological process; CC, Cellular component; GO, Gene ontology; KEGG, Kyoto Encyclopedia of Genes and Genomes. Bars, means \pm SD of experimental triplicates.

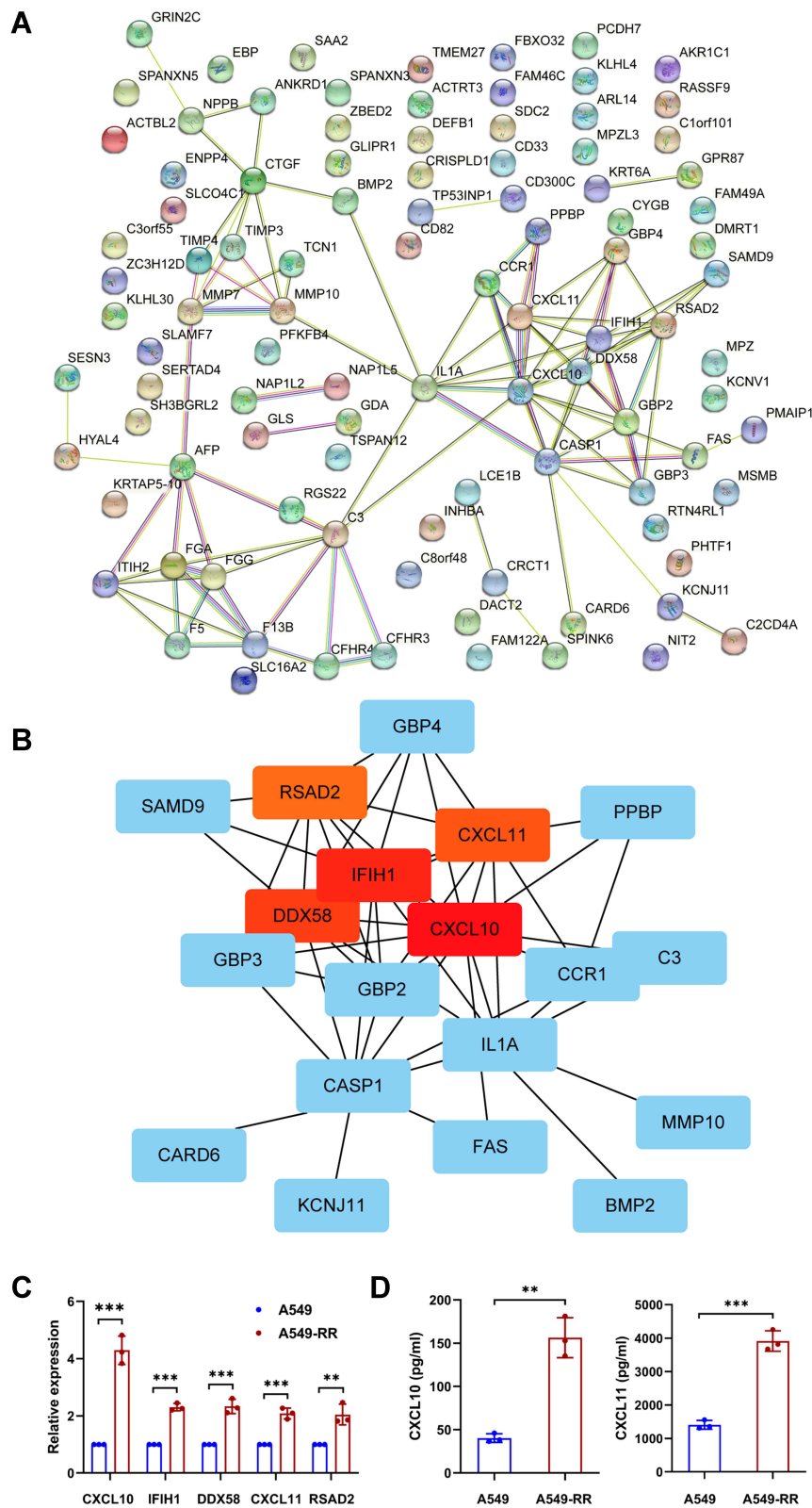


Figure 3 Identification and validation of hub genes. **(A)** The PPI network was analyzed by String software. **(B)** Identified the hub gene by Cytohubba. CXCL10, IFIH1, DDX58, CXCL11, RSAD2 were calculated as the top 5 hub genes. **(C)** Different expression of the top 5 hub genes in cases and controls verified using qRT-PCR. **(D)** The relative expression of cytokine in case and control groups using ELISA. Each experiment consisted of three biological replicates. ** $p < 0.01$, *** $p < 0.001$. **Abbreviations:** PPI, protein–protein interaction. qRT-PCR, Quantitative Real-time PCR. ELISA, enzyme linked immunosorbent assay.

Validation of Hub Genes

Based on the results of microarray analysis, the expression of the above five hub genes were further confirmed by qRT-PCR. Consistent with microarray analysis, statistically significant differences were found between case and control samples ($p < 0.05$) (Figure 3C). ELISA was performed to reveal the expression level of cytokines including CXCL10 and CXCL11. As the results shown in Figure 3D, the levels of CXCL10 ($p = 0.0011$) and CXCL11 ($p = 0.0002$) in A549-RR were significantly higher than that in A549.

Analysis of Immune Infiltration

Tumor-infiltrating immune cells play an indispensable role in tumor microenvironment and are also correlated to tumor genesis, development and metastasis.¹⁷ Among the five hub genes, CXCL10 and CXCL11 are well known to activate CD8+ T cells. In this study, TIMER, MCPOUNTER, Cibersort-ABS, QUANTISEQ and XCELL algorithms were used to estimate the relationship between CD8+ T cell infiltration and the five hub genes in different types of TCGA tumors. Interestingly we found a statistically positive correlation between hub gene and CD8+ T cell infiltration in lung adenocarcinoma based on all or most algorithms (Figure 4A and B).

Verification of Immune Infiltration

As the immune infiltration analysis showed that up-regulated hub genes in A549-RR were significantly associated with CD8+ T cell infiltration. Therefore, flow cytometry was further performed to verify the chemotaxis of radiotherapy resistant cells to CD8+ T cells. The results revealed that A549-RR had improved CD8+ T cells chemotaxis ($p = 0.0073$) (Figure 4C and D).

ChIP-X Enrichment Analysis

ChIP-X Enrichment Analysis revealed that these hub genes could be regulated by the same transcription factors, combined with rank and mean rank as suggested, STAT1 is likely to be a transcription factor of these hub genes. (Table 2).

Inhibition of STAT1 Could Improve the Therapeutic Efficacy of Radiotherapy

Among the transcription factors that fit the criteria, STAT1 has mostly been reported to be correlated with radiation resistance in variety of tumors. As shown in Figure 5A and B, phosphorylated STAT1 (Y701) especially the α -subunit was significantly activated in A549-RR, suggesting that STAT1 signaling pathway plays a role in radiotherapy resistance of NSCLC. As shown in Figure 5C, upregulation of PD-L1 was also found in our radiotherapy resistant group, which was consistent with the previous microarray analysis. Figure 5D further verified the level of PD-L1 expression using immunoblotting and Figure 5E was the quantification of PD-L1 expression. To explore the effect of STAT1 on radiotherapy resistance, we used A549RR, the radiotherapy resistant cell line, and found that STAT1 inhibitor could significantly improve the sensitivity of radiotherapy (Figure 5F–H).

Discussion

Radiation induced DNA damage repair, cell cycle disorder, characterization of cancer stem cells and epithelial mesenchymal transformation are the main causes of tumor radiation resistance. At present, the mechanism of radiotherapy resistance remains to be further elucidated. Hence, it is particularly important to investigate the mechanism of reversing radiation resistance and explore markers that improve radiotherapy sensitivity and reduce metastasis and recurrence of NSCLC due to radiation resistance.

In our study, compared with the control group, 390 up regulated DEGs in the radiotherapy resistance group were mostly enriched in cytokine-cytokine receptor interaction signaling pathway, which suggested dysregulation of immune cell in radiotherapy resistance group. According to CytoHubba analysis, CXCL10, IFIH1, DDX58, CXCL11, RSAD2 were the most significant hub genes of DEGs. To further verify the RNA microarray results, we validated the expression level of the five hub genes by qRT-PCR. The results were consistent with those of RNA microarray.

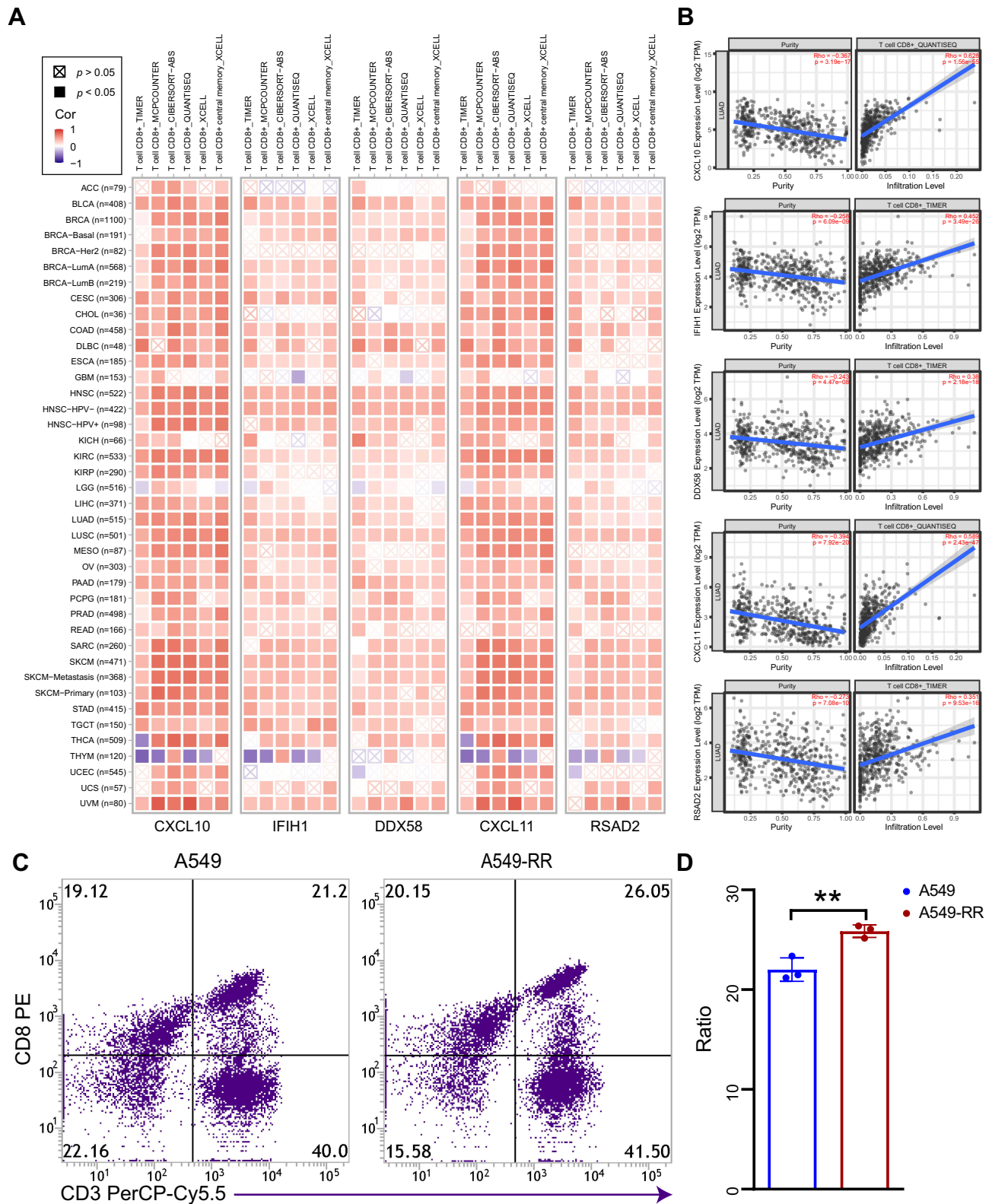


Figure 4 Correlation analysis between hub genes expression and immune infiltration of CD8+T cell. **(A)** Different algorithms were performed to explore the relationship between the expression level of the hub genes and the infiltration level of CD8+T cell across all types of cancer in TCGA. **(B)** The scatterplot data of the lung adenocarcinoma produced using one algorithm. **(C)** The chemotaxis of CD8+T cell between case and control group were detected by flow cytometry. **(D)** Quantification of data in C. Each experiment consisted of three biological replicates. ****** $p < 0.01$.

Abbreviation: TCGA, The Cancer Genome Atlas.

Table 2 ChIP-X Enrichment Analysis Results

Rank	TF	Mean Rank	Overlapping Genes	Library
1	BATF2	8	5	ARCHS4 Coexpression, 9; Enrichr Queries, 3; GTEx Coexpression, 12 Literature ChIP-seq, 131; ARCHS4
7	STAT1	29	5	Coexpression, 2; ENCODE ChIP-seq, 2; Enrichr Queries, 4; ReMap ChIP-seq, 3; GTEx Coexpression, 32
50	RELB	210	5	ARCHS4 Coexpression, 23; Enrichr Queries, 14; ReMap ChIP-seq, 1; GTEx Coexpression, 802
85	ETV7	254.7	5	ARCHS4 Coexpression, 1; Enrichr Queries, 1; GTEx Coexpression, 762
258	SPI10	433.3	5	ARCHS4 Coexpression, 1052; Enrichr Queries, 2; GTEx Coexpression, 246
413	SPI40	531	5	ARCHS4 Coexpression, 1198; Enrichr Queries, 5; GTEx Coexpression, 390

CXCL10 and CXCL11 are angiogenic chemokines, those antimicrobial genes encode a CXC subfamily chemokine and a ligand for the CXCR3 receptor. Binding of this protein to CXCR3 causes pleiotropic effects such as monocyte stimulation, migration of natural killer and T-cell, and adhesion molecule expression modulation.^{18,19} In melanoma, renal, and colon cell carcinomas, CXCL10 predicted stronger metastatic potential and was significantly correlated with poor overall survival and early metastatic disease progression.²⁰ Ionizing radiation has the potential to increase CXCL10 expression,²¹ and CXCL10 was proved to be a potential target for response of radiotherapy in patients with tongue squamous cell carcinoma,²² indicated the potential role of CXCL10 in modulating radiosensitivity and the possibility of reversing radiotherapy resistance by targeting CXCL10. CXCL11 has stronger CXCR3 affinity and may help to promote cancer growth.²³ CXCL11, in addition to CXCR3, may bind to CXCR7, which was associated with tumor invasiveness and reduced apoptosis,²⁴ and inhibition of CXCL11/CXCR7 axis could block glioblastoma multiforme recurrence after irradiation.²⁵ In our study, expression of CXCL10 and CXCL11 were elevated in radiotherapy resistant group, suggested that the disturbance of immune system may play a role in the resistance to radiotherapy.

Retinoic-acid-inducible gene I(RIG-I)-like receptors (RLRs), including DDX58 and IFIH1, work in the process of cytoplasmic viral components recognition and mitochondrial signaling adaptor activation, which provides the platform recruiting downstream kinases and finally leads to the stimulation of IFN signaling pathways,^{26–29} so as to initiate the innate immune response.³⁰ Activation of IFN signaling pathway has been reported to be related to radiotherapy resistance in colorectal cancer.^{7,31} In addition, targeting RLRs, including DDX58 and IFIH1, may improve the sensitivity to radiation therapy of variety tumors.³² In our study, consistent with microarray results, DDX58 and IFIH1 were significantly upregulated in radiotherapy resistant cell lines, suggesting the potential roles of DDX58 and IFIH1 as tumor therapeutic targets, especially in improving radiotherapy sensitivity.

RSAD2 has been reported to be overexpressed in breast cancer and melanoma, and could be used as a prognostic factor.^{32–34} The protein encoded by this gene could be induced by interferon and activated in the response of antiviral and innate immune. Studies of the interaction between host immune system and radiation therapy have revealed new mechanisms that may be used to improve the efficacy of radiotherapy.^{35,36} Radiation promotes the release of chemokines that recruit inflammatory cells into TME. Cytokines could dose-dependently influence ionizing radiation responses through their pleiotropy, aggressiveness, and fibrosis.³⁷ Several immune-related genes were screened from radiotherapy resistance group in our study which involved in cytokine-cytokine receptor interaction. It suggested that the balance of proinflammatory and anti-inflammatory cytokines is a key factor to determine the resistance of radiotherapy.

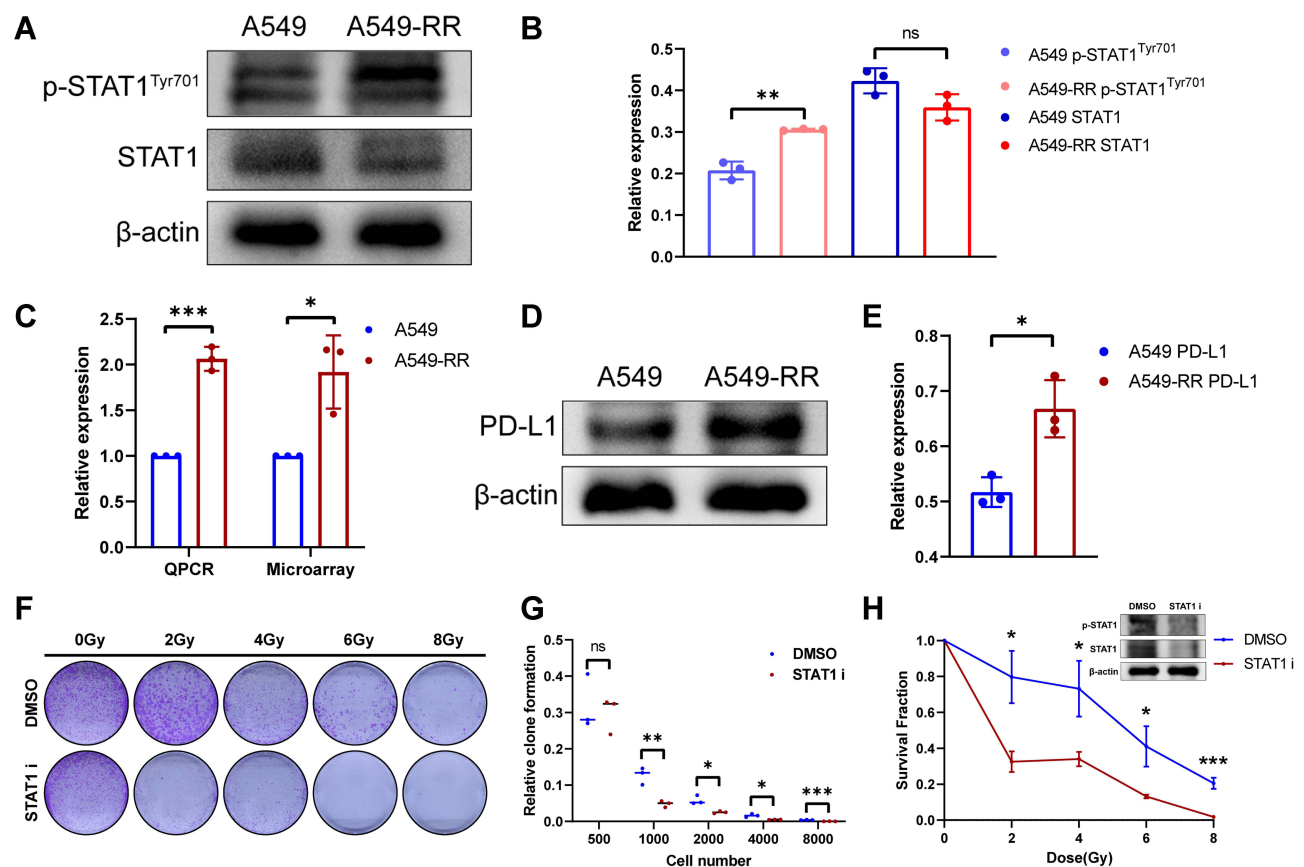


Figure 5 Effects of STAT1 inhibitor on radiotherapy resistance. (A) The expression levels of total STAT1 and p-STAT1 (Y701). (B) Relative expression of STAT1 and p-STAT1. (C) Relative expression of PD-L1. (D) The expression levels of PD-L1. (E) Quantification of PD-L1 expression. (F) A549-RR cells were planted and incubated with STAT1 inhibitor (S1491, Selleck, 2μg/mL, 24h) followed by radiotherapy and then cultured for 2 weeks. (G) Clone formation rate according to D, the results were calculated according to the ratio of clone number to inoculated cell number. (H) Survival fraction according to D. **p* < 0.05, ***p* < 0.01, ****p* < 0.001. Abbreviation: ns, no significance.

Based on ChIP-X enrichment analysis, the smaller mean rank is, the higher the certainty of prediction is. Considering that BATF2 plays a role as a tumor suppressor gene in cancers^{38,39} and has not been reported to be associated with radiation resistance, the overall ranking of other transcription factors in Table 2 is much lower than that of STAT1, we suspected that those hub genes were likely to be promoted by STAT1, which ranking the second place among those transcription factors. Unlike the other STAT isoforms, STAT1 was reported to be the major transcription factor that work as a therapeutic target in radioresistance among many types of cancer cells.^{8–11} However, the potential function of STAT1 in radiotherapy resistance of lung cancer has not yet been reported. It had previously been reported that high levels of persistently activated STAT1 are required for cell survival following ionizing radiation,⁴⁰ STAT1 activation may result in tumor radiation adaptation by directly affecting tumor cell cellular transduction. Immunoblotting showed that phosphorylated STAT1 (Y701) especially the α -subunit was significantly activated after radiation resistance. As STAT1 α is a latent cytoplasmic transcription factor activated in response to IFN- γ , suggested IFN/STAT1 activation might triggers radioresistant properties in NSCLC cancer, which had been reported before.⁷

Aside from cancer cells, radiotherapy has the potential to alter the balance of tumor promoting and tumor suppressing cells. Inflammatory signaling pathways are activated after radiotherapy by stimulating cellular survival pathways and the innate immune system,^{35,36,41} which was consistent with our results. In addition to affecting the immune microenvironment, radiotherapy also activates STAT1 signaling pathway. It had been reported that STAT1 activation increases PD-L1 expression in a variety of tumors,^{42–44} upregulation of PD-L1 was also found in our radiotherapy resistant group. Furthermore, our results showed the blockade of PD-L1 enhances the therapeutic efficacy of radiotherapy. These results suggested that although radiotherapy promotes the release of immune-promoting cytokines from tumor cells, the

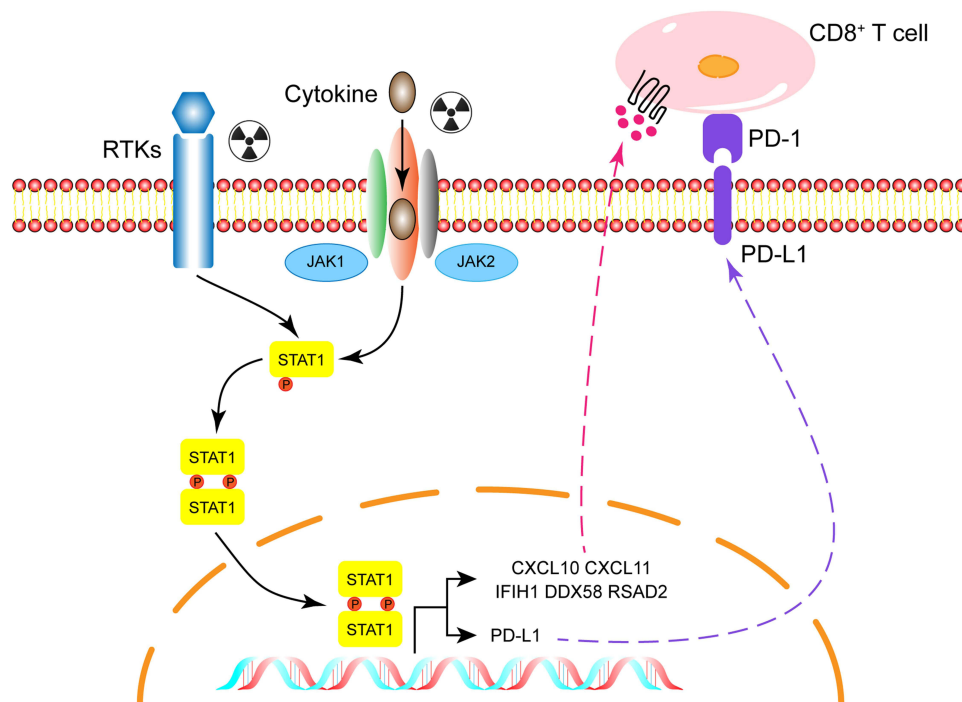


Figure 6 Diagram of potential mechanisms of radiation resistance.

Abbreviation: RTKs, receptor tyrosine kinases.

upregulation of PD-L1 ultimately leads to the exhaustion of anti-tumor immunity, as we described in Figure 6, suggested the main mechanism of radioresistance may be depletion of anti-tumor immunity and combined immunotherapy could improve radiotherapy sensitivity as well as against radiation resistance.

Though we identified five hub genes in radioresistance group using bioinformatic analysis, our study only focused on the cellular level. Hence, our conclusions still need further exploration.

Conclusion

Although immune system activation occurs followed by radiation resistance, we hypothesized that the upregulation of PD-L1 expression caused by STAT1 activation might be one of the mechanisms of radiotherapy resistance.

Abbreviations

NSCLC, non-small cell lung cancer; SCLC, small cell lung cancer; DEGs, differentially expressed genes; GO, Gene ontology; KEGG, Kyoto Encyclopedia of Genes and Genomes; GSEA, Gene Set Enrichment Analysis; PPI, protein-protein interaction; BP, biological process; CC, cytological component; MF, molecular function; TME, tumor microenvironment.

Data Sharing Statement

The datasets presented in this study can be found in GEO database, the GEO accession number was: GSE197236.

Ethics Approval

The human blood samples used in this study were approved by the Medical Ethics Committee of Sun Yat-sen Memorial Hospital, Sun Yat-sen University (Approval No.SYSEC-KY-KS-2022-053).

Acknowledgments

We would like to thank all participants in this study.

Funding

This work was supported by grants from the Natural Science Foundation of China (82002823, 82025026, 81730077), Program from Guangdong Basic and Applied Basic Research Foundation (2019A1515110082), Guangdong Science and Technology Department (2020B1212060018, 2020B1212030004).

Disclosure

The authors report no conflicts of interest in this work.

References

1. Wang Z, Huang Y, Zhang J. Molecularly targeting the PI3K-Akt-mTOR pathway can sensitize cancer cells to radiotherapy and chemotherapy. *Cell Mol Biol Lett*. 2014;19(2):233–242. doi:10.2478/s11658-014-0191-7
2. Vitale I, Manic G, De Maria R, Kroemer G, Galluzzi L. DNA damage in stem cells. *Mol Cell*. 2017;66(3):306–319.
3. Iqbal MA, Arora S, Prakasam G, Calin GA, Syed MA. MicroRNA in lung cancer: role, mechanisms, pathways and therapeutic relevance. *Mol Aspects Med*. 2019;70:3–20. doi:10.1016/j.mam.2018.07.003
4. Zhu L, Xue F, Xu X, et al. MicroRNA-198 inhibition of HGF/c-MET signaling pathway overcomes resistance to radiotherapy and induces apoptosis in human non-small-cell lung cancer. *J Cell Biochem*. 2018;119(9):7873–7886. doi:10.1002/jcb.27204
5. Barker HE, Paget JT, Khan AA, Harrington KJ. The tumour microenvironment after radiotherapy: mechanisms of resistance and recurrence. *Nat Rev Cancer*. 2015;15(7):409–425. doi:10.1038/nrc3958
6. Wu CT, Chen MF, Chen WC, Hsieh CC. The role of IL-6 in the radiation response of prostate cancer. *Radiat oncol*. 2013;8:159. doi:10.1186/1748-717X-8-159
7. Liu S, Imani S, Deng Y, et al. Targeting IFN/STAT1 pathway as a promising strategy to overcome radioresistance. *Oncotargets Ther*. 2020;13:6037–6050. doi:10.2147/OTT.S256708
8. Weichselbaum RR, Ishwaran H, Yoon T, et al. An interferon-related gene signature for DNA damage resistance is a predictive marker for chemotherapy and radiation for breast cancer. *Proc Natl Acad Sci U S A*. 2008;105(47):18490–18495. doi:10.1073/pnas.0809242105
9. Khodarev NN, Beckett M, Labay E, Darga T, Roizman B, Weichselbaum RR. STAT1 is overexpressed in tumors selected for radioresistance and confers protection from radiation in transduced sensitive cells. *Proc Natl Acad Sci U S A*. 2004;101(6):1714–1719. doi:10.1073/pnas.0308102100
10. Fryknäs M, Dhar S, Oberg F, et al. STAT1 signaling is associated with acquired crossresistance to doxorubicin and radiation in myeloma cell lines. *Int J Cancer*. 2007;120(1):189–195. doi:10.1002/ijc.22291
11. Hui Z, Tretiakova M, Zhang Z, et al. Radiosensitization by inhibiting STAT1 in renal cell carcinoma. *Int J Radiat Oncol Biol Phys*. 2009;73(1):288–295. doi:10.1016/j.ijrobp.2008.08.043
12. Deng L, Liang H, Burnette B, et al. Irradiation and anti-PD-L1 treatment synergistically promote antitumor immunity in mice. *J Clin Invest*. 2014;124(2):687–695. doi:10.1172/JCI67313
13. Dovedi SJ, Adlard AL, Lipowska-Bhalla G, et al. Acquired resistance to fractionated radiotherapy can be overcome by concurrent PD-L1 blockade. *Cancer Res*. 2014;74(19):5458–5468. doi:10.1158/0008-5472.CAN-14-1258
14. Chen Y, Gao M, Huang Z, Yu J, Meng X. SBRT combined with PD-1/PD-L1 inhibitors in NSCLC treatment: a focus on the mechanisms, advances, and future challenges. *J Hematol Oncol*. 2020;13(1):105. doi:10.1186/s13045-020-00940-z
15. Chin CH, Chen SH, Wu HH, Ho CW, Ko MT, Lin CY. cytoHubba: identifying hub objects and sub-networks from complex interactome. *BMC Syst Biol*. 2014;8 Suppl 4(Suppl4):S11. doi:10.1186/1752-0509-8-S4-S11
16. Keenan AB, Torre D, Lachmann A, et al. ChEA3: transcription factor enrichment analysis by orthogonal omics integration. *Nucleic Acids Res*. 2019;47(W1):W212–w224. doi:10.1093/nar/gkz446
17. Fridman WH, Galon J, Dieu-Nosjean MC, et al. Immune infiltration in human cancer: prognostic significance and disease control. *Curr Top Microbiol Immunol*. 2011;344:1–24.
18. Wennerberg E, Kremer V, Childs R, Lundqvist A. CXCL10-induced migration of adoptively transferred human natural killer cells toward solid tumors causes regression of tumor growth in vivo. *Cancer Immunol Immunother*. 2015;64(2):225–235. doi:10.1007/s00262-014-1629-5
19. Utsumi T, Suyama T, Imamura Y, et al. The association of CXCR3 and renal cell carcinoma metastasis. *J Urol*. 2014;192(2):567–574. doi:10.1016/j.juro.2014.01.100
20. Wightman SC, Uppal A, Pitroda SP, et al. Oncogenic CXCL10 signalling drives metastasis development and poor clinical outcome. *Br J Cancer*. 2015;113(2):327–335.
21. Lin Y, Lu R, Hou J, Zhou GG, Fu W. IFN γ -inducible CXCL10/CXCR3 axis alters the sensitivity of HEp-2 cells to ionizing radiation. *Exp Cell Res*. 2021;398(1):112382. doi:10.1016/j.yexcr.2020.112382
22. Rentoft M, Coates PJ, Loljung L, Wilms T, Laurell G, Nylander K. Expression of CXCL10 is associated with response to radiotherapy and overall survival in squamous cell carcinoma of the tongue. *Tumour Biol*. 2014;35(5):4191–4198. doi:10.1007/s13277-013-1549-6
23. Tokunaga R, Zhang W, Naseem M, et al. CXCL9, CXCL10, CXCL11/CXCR3 axis for immune activation - A target for novel cancer therapy. *Cancer Treat Rev*. 2018;63:40–47. doi:10.1016/j.ctrv.2017.11.007
24. Burns JM, Summers BC, Wang Y, et al. A novel chemokine receptor for SDF-1 and I-TAC involved in cell survival, cell adhesion, and tumor development. *J Exp Med*. 2006;203(9):2201–2213. doi:10.1084/jem.20052144
25. Walters MJ, Ebsworth K, Berahovich RD, et al. Inhibition of CXCR7 extends survival following irradiation of brain tumours in mice and rats. *Br J Cancer*. 2014;110(5):1179–1188. doi:10.1038/bjc.2013.830
26. Xu LG, Wang YY, Han KJ, Li LY, Zhai Z, Shu HB. VISA is an adapter protein required for virus-triggered IFN-beta signaling. *Mol Cell*. 2005;19(6):727–740. doi:10.1016/j.molcel.2005.08.014
27. Kawai T, Takahashi K, Sato S, et al. IPS-1, an adaptor triggering RIG-I- and Mda5-mediated type I interferon induction. *Nat Immunol*. 2005;6(10):981–988. doi:10.1038/ni1243

28. Seth RB, Sun L, Ea CK, Chen ZJ. Identification and characterization of MAVS, a mitochondrial antiviral signaling protein that activates NF-kappaB and IRF 3. *Cell*. 2005;122(5):669–682. doi:10.1016/j.cell.2005.08.012
29. Meylan E, Curran J, Hofmann K, et al. Cardif is an adaptor protein in the RIG-I antiviral pathway and is targeted by hepatitis C virus. *Nature*. 2005;437(7062):1167–1172. doi:10.1038/nature04193
30. Chow KT, Gale M, Loo YM. RIG-I and Other RNA Sensors in Antiviral Immunity. *Annu Rev Immunol*. 2018;36:667–694. doi:10.1146/annurev-immunol-042617-053309
31. Chen B, Alvarado DM, Iticovici M, et al. Interferon-induced IDO1 mediates radiation resistance and is a therapeutic target in colorectal cancer. *Cancer Immunol Res*. 2020;8(4):451–464. doi:10.1158/2326-6066.CIR-19-0282
32. Rehwinkel J, Gack MU. RIG-I-like receptors: their regulation and roles in RNA sensing. *Nat Rev Immunol*. 2020;20(9):537–551. doi:10.1038/s41577-020-0288-3
33. Tang J, Yang Q, Cui Q, et al. Weighted gene correlation network analysis identifies RSAD2, HERC5, and CCL8 as prognostic candidates for breast cancer. *J Cell Physiol*. 2020;235(1):394–407. doi:10.1002/jcp.28980
34. Jessen C, Krefß JKC, Baluapuri A, et al. The transcription factor NRF2 enhances melanoma malignancy by blocking differentiation and inducing COX2 expression. *Oncogene*. 2020;39(44):6841–6855. doi:10.1038/s41388-020-01477-8
35. Burnette BC, Liang H, Lee Y, et al. The efficacy of radiotherapy relies upon induction of type I interferon-dependent innate and adaptive immunity. *Cancer Res*. 2011;71(7):2488–2496. doi:10.1158/0008-5472.CAN-10-2820
36. Gupta A, Probst HC, Vuong V, et al. Radiotherapy promotes tumor-specific effector CD8+ T cells via dendritic cell activation. *J Immunol*. 2012;189(2):558–566. doi:10.4049/jimmunol.1200563
37. Kim BM, Hong Y, Lee S, et al. Therapeutic implications for overcoming radiation resistance in cancer therapy. *Int J Mol Sci*. 2015;16(11):26880–26913. doi:10.3390/ijms161125991
38. Xie JW, Huang XB, Chen QY, et al. m(6)A modification-mediated BATF2 acts as a tumor suppressor in gastric cancer through inhibition of ERK signaling. *Mol Cancer*. 2020;19(1):114. doi:10.1186/s12943-020-01223-4
39. Wang Q, Lu W, Yin T, Lu L. Calycosin suppresses TGF-β-induced epithelial-to-mesenchymal transition and migration by upregulating BATF2 to target PAI-1 via the Wnt and PI3K/Akt signaling pathways in colorectal cancer cells. *J Exp Clin Cancer Res*. 2019;38(1):240. doi:10.1186/s13046-019-1243-7
40. Khodarev NN, Roizman B, Weichselbaum RR. Molecular pathways: interferon/stat1 pathway: role in the tumor resistance to genotoxic stress and aggressive growth. *Clin Cancer Res*. 2012;18(11):3015–3021. doi:10.1158/1078-0432.CCR-11-3225
41. Takeuchi O, Akira S. Pattern recognition receptors and inflammation. *Cell*. 2010;140(6):805–820. doi:10.1016/j.cell.2010.01.022
42. Garcia-Diaz A, Shin DS, Moreno BH, et al. Interferon receptor signaling pathways regulating PD-L1 and PD-L2 expression. *Cell Rep*. 2017;19(6):1189–1201. doi:10.1016/j.celrep.2017.04.031
43. Chen S, Crabill GA, Pritchard TS, et al. Mechanisms regulating PD-L1 expression on tumor and immune cells. *J Immunother Cancer*. 2019;7(1):305. doi:10.1186/s40425-019-0770-2
44. Lv H, Lv G, Chen C, et al. NAD(+) metabolism maintains inducible PD-L1 expression to drive tumor immune evasion. *Cell Metab*. 2021;33(1):110–127.e115. doi:10.1016/j.cmet.2020.10.021